

Heating/melting of a fused silica particle by convection and radiation

C.C. Tseng, R. Viskanta *

Heat Transfer Laboratory, School of Mechanical Engineering, Purdue University, West Lafayette, IN 47907, USA

Received 11 July 2005; received in revised form 21 January 2006

Available online 18 April 2006

Abstract

The effect of internal absorption and emission of radiation on the heating/melting process of small fused silica particles is analyzed. The particle is considered to be semitransparent to radiation, and the radiative transfer theory is used to predict the local volumetric absorption/emission rate. The transient energy equation with conduction and radiation accounted for is solved to predict the temperature distribution in the particle and the solid–liquid interface position after the melting has started. The radiative transfer calculations are carried out on the spectral basis using published spectral optical property data for fused silica. Results of parametric calculations for different diameter particles, surroundings temperatures and external flow conditions are reported and discussed.

© 2006 Elsevier Ltd. All rights reserved.

Keywords: Radiation effects; Semitransparent particle; Phase change

1. Introduction

The heating and melting of particles is encountered in a very broad range of industrial applications. Examples include spray coating processes using plasma to heat and melt suspended particles [1], feeding of silicon pellets into a melt pool to produce crystal products [2], laser melting of gold particles in nanoscale [3], manufacturing of steel [4] and others. In all of these applications absorption of radiation has not been considered or radiation was treated only as a surface phenomenon. Of particular interest in this study is the theoretical investigation of the relative importance of radiative heat transfer on the heating/melting of a semitransparent particle.

Many man-made and technologically important materials such as glass, crystals, fused silica (SiO_2) are semitransparent to radiation [5,6]. When analyzing the heating/melting of such particles by convection and radiation not only heat conduction in the interior of the particle but volumetric absorption/emission of radiation need to be con-

sidered. Typically, the raw materials are melted in beds, but there are also situations where preforms are being melted. Since most of the semitransparent materials are highly selective and have high melting temperatures, correct treatment of radiative transfer is critical in predicting the melting dynamics. To gain fundamental understanding of the phenomena, the focus of the discussion is on melting of a single isolated particle rather than of the bed.

The main difference between the present problem and those discussed in the literature is that the contribution to the irradiance by the external radiation sources, and the internal emission by the matter needs to be considered at higher particle temperature. As a concrete example, we consider fused silica as a typical material to perform the simulations, because it has a high and unique melting temperature. Also, the thermophysical and radiative properties are available in the literature, and the material is very important technologically.

Liquid melt produced at the phase change interface may or may not be removed. This condition depends on the surface tension at the liquid–gas interface and the gravitational body force acting on the melt. Even through the surface tension can support the liquid for a wide range of droplet diameters, it can no longer support the droplet

* Corresponding author. Tel.: +1 765 494 5632; fax: +1 765 494 0539.
E-mail address: viskanta@ecn.purdue.edu (R. Viskanta).

Nomenclature

c	specific heat (J/kg K)	λ	wavelength (μm)
D	particle diameter (m)	ρ	density (kg/m^3) or reflectivity (–)
G	irradiance (W/m^2)	τ	transmissivity (–)
Δh_f	latent heat of fusion (J/kg)	τ_d	optical diameter, κD , (–)
I	intensity ($\text{W/m}^2 \mu\text{m}$)	ϕ	porosity (–)
k	thermal conductivity (W/m K) or absorption index (–)	ψ	angle (rad)
l	optical geometric function (m)		
n	refractive index (–)	<i>Superscripts</i>	
R	particle radius (m)	o	refers to external
r	radius coordinate (m)	–	refers to mean value
T	temperature (K)	<i>Subscripts</i>	
t	time (s)	ext	refers to external
		f	refers to fusion
<i>Greek symbols</i>		g	refers to gas
α	absorptance or absorptivity (–)	int	refers to internal
β	angle (rad)	m	refers to melt
ϵ	emissivity (–)	s	refers to solid
ζ	dimensionless radius, r/R (–)	sur	refers to surroundings
θ	angle (rad)	λ	refers to spectral value
κ	absorption coefficient $4\pi k/\lambda$, ($1/\text{m}$)		

when the critical value of the surface tension has been exceeded. The surface tension for SiO_2 (1883 K) is not constant but depends on the surface temperature and is given by Fujino et al. [7]. The results of available calculations [8] reveal that for a droplet of SiO_2 melt with the diameter greater than 5.5 mm, the liquid would no longer be supported by the surface tension at the fusion temperature. This means that when melting small SiO_2 particles for which the diameter is smaller than 5 mm, two interface conditions are needed to describe the melting process; one is for the liquid–gas interface and another is just for the solid–liquid interface.

The relative importance of radiation absorption on enhancing the heating/melting processes of a semitransparent spherical particle exposed to external radiation is not fully understood. For example, under what conditions and to what level of detail is it necessary to consider radiative transfer when heating/melting a semitransparent particle exposed to radiation? And to what level of detail? Would neglect of radiation (i.e., assuming the particle is transparent to radiation) or treating the particle as semitransparent to radiation and use radiative transfer theory to predict [6] local volumetric absorption/emission rate be required? In addition, since the spectrum of medium may have weakly (semitransparent or transparent) and strongly (opaque) absorbing bands, is it possible to identify an optimum heating source (surroundings temperature) for heating the medium? The purpose of the paper is to develop a radiative transfer model for heating/melting of a suspended (isolated) semitransparent particle which is exposed to irradiation from an external source. The model is then

combined with a thermal energy model to examine the relative importance of radiative transfer vs. convection on the heating/melting process, and the predictions are compared with those based on simplified models.

2. Analysis

Rigorous treatment of heating of a polydisperse cloud of particles by convection and radiation, with phase change taking place, is exceeding complex and does not appear to have been analyzed. In order to make the analysis more treatable, we consider a single, isolated particle and focus on its convective and radiative heating. The interaction between particle and the external gas flow is not considered. Convection is treated parametrically by prescribing the heat transfer coefficient. External radiation incident on the particle is also treated parametrically by assuming the radiation field (intensity) incident on the outside of the particle originates from sources (i.e., walls of the “enclosure” and ambient gas/particle mixture) at an effective surroundings temperature T_{sur} . The incident radiation intensity is assumed to be isotropic (i.e., independent of direction).

We assume that an isolated semitransparent spherical particle is initially at its ambient temperature, and then it is suddenly placed in a high temperature environment to be heated by convection and radiation (Fig. 1). The melting of the material begins when the surface temperature reaches the fusion temperature. Thus, the time period before the particle begins to melt is referred as the heating period, followed by the melting period. For the purpose of

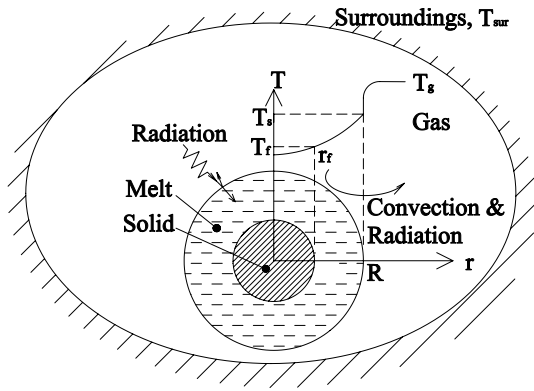


Fig. 1. Schematic representation of semitransparent particle heating/melting.

simplicity, the following assumptions are made in this analysis: (1) heat conduction and radiation are one-dimensional; (2) radiative heat transfer is of quasi-steady-state; (3) the particle is spherical in shape, and its diameter is much larger than the wavelength of radiation; (4) sublimation of the solid-phase and evaporation of the melt are neglected; (5) melting occurs at the solid/liquid interface; (6) the interface is optically smooth and remains at a known constant melting temperature after the particle has been heated to this temperature; (7) intensity of radiation incident on the particle is independent of direction and comes from a black body source at temperature T_{sur} ; (8) the particle is homogeneous and scattering is negligible in comparison to absorption; (9) the liquid melt produced during the phase change is assumed to remain surrounding the solid. The idealizations made are reasonable. Assumption three can be relaxed by considering polarization of radiation [9,10]. Flow and drag on the particle may cause it to lose its spherical shape (Assumption 4), but the distortion of the melt shape from a spherical shell is not considered to be serious for small particles. The gravitational force would tend to distort the melt surrounding the solid-phase, but the surface tension force would oppose it. Analysis has shown [8] that a fused silica droplet with a diameter greater than 5.5 mm is no longer supported by the surface tension, and the melt would be distorted from the spherical shape (Assumption 9).

Particles are heated from the ambient temperature to the fusion temperature, and the process can be separated into two time regimes. The time regime before the surface temperature reaches the fusion temperature is referred to as heating period. After the heating period and when the particle begins melting, the time regime is referred to as the melting period. The two time regimes are analyzed separately.

During the heating period of a semitransparent particle, conduction and radiation are the only two modes of heat transfer. The one-dimensional transient energy equation for heating of a spherical particle capable of absorbing and emitting radiation is

$$\rho_i c_i \frac{\partial T_i}{\partial t} = \frac{1}{r^2} \frac{\partial}{\partial r} \left(k_i r^2 \frac{\partial T_i}{\partial r} \right) - \int_0^\infty \kappa_\lambda [4\pi n_\lambda^2 I_{b,\lambda}(T_i) - G_{\lambda,i}(r,t)] d\lambda, \quad i = s, m. \quad (1)$$

In the equation, s and m represent for the solid and the melt, respectively. The spectral irradiance $G_{\lambda,i}$ is defined by [6]

$$G_{\lambda,i}(r,t) \equiv \int_{4\pi} I_{\lambda,i}(r,\theta,\phi,t) d\Omega = 2\pi \int_{-1}^1 I_{\lambda,i}(r,\mu,t) d\mu. \quad (2)$$

The first term on the right-hand-side of Eq. (1) accounts for heat conduction, and the second term represents the radiative transfer [6]. The spectral radiance (intensity of radiation) along a pencil of rays in spherical coordinates for non-scattering semitransparent material is calculated from the radiative transfer equation. The direction cosine (μ) is of the angle (θ) between the radius vector (\hat{r}) and the direction vector (\hat{s}) of the radiation beam. During the heating period (before the particle starts melting) only the solid-phase energy equation is solved, but after melting starts both the solid and liquid phase equations are solved.

During the preheating period, the heat transfer rate across the interface is balanced by conduction, convection, and surface radiation. Thus, the energy equation, Eq. (1), is subject to the following boundary condition, at the surface ($r = R$):

$$k_i \left. \frac{\partial T_i}{\partial r} \right|_{r=R} = \bar{h}(T_g - T_{\text{surface}}) + \pi \int_{\Delta\lambda_{\text{op}}} \alpha_\lambda I_\lambda^o d\lambda - \pi \int_{\Delta\lambda_{\text{op}}} \epsilon_\lambda I_{b,\lambda}(T_{\text{surface}}) d\lambda, \quad i = s, m. \quad (3)$$

The first term on the right-hand-side of this equation accounts for convection. The average heat transfer coefficient is calculated from the recommended correlation [11,12]. The second term represents the incident radiation absorbed at the surface in the cutoff wavelength range $\Delta\lambda_{\text{op}}$ in which the particle is considered to be opaque to radiation. The third term represents emission of radiation from the surface in the opaque part of the spectrum. In the equation I_λ^o represents the intensity of radiation emitted by the surroundings, i.e., $I_\lambda^o = I_{b,\lambda}(T_{\text{sur}})$, and incident on the particle. The absorptance α_λ and the emittance ϵ_λ in Eq. (3) are assumed to be the same, i.e., $\alpha_\lambda = \epsilon_\lambda$, following Kirchhoff's Law. Additional details for determining the absorptance are provided in the section to follow. At the center of the particle the temperature profile is symmetric, and initially the temperature of the particle is assumed to be uniform.

After the particle starts melting at the phase change interface, $r = r_f(t)$, the energy balance is given by

$$\rho_s \Delta h_f \left. \frac{\partial r}{\partial t} \right|_{r=r_f} = k_s \left. \frac{\partial T_s}{\partial r} \right|_{r=r_f^-} - k_m \left. \frac{\partial T_m}{\partial r} \right|_{r=r_f^+}, \quad (4)$$

where Δh_f is the latent heat of fusion. Of course, the particle is assumed to change phase at a definite fusion temperature T_f .

It is assumed that the phase change of the particle (considered to be homogeneous and without any microscopic inclusions) occurs at the interface, and the material melts at the fusion temperature. Internal melting, even though the temperature of the solid-phase may exceed the fusion temperature owing to the internal deposition of radiant energy, is excluded from consideration [13].

3. Radiative transfer

To make the problem tractable mathematically and gain fundamental understanding of radiative transfer, a mono-disperse semitransparent particle is considered. The focus is on the deposition (absorption) of radiation originating from the surroundings. Thermal and radiative interaction between the particle and the external gaseous flow field, if any, is neglected. The particle is placed in an environment in which the gas composition and temperature do not change with time (Fig. 1). The effect of radiation is modeled parametrically by imposing a blackbody effective temperature of the surroundings T_{sur} , which may consist of the surrounding walls and radiating gases/particles mixture.

The nature of the heating/melting of particles cannot be considered as either opaque or transparent but must be treated as being semitransparent to radiation. The radiation field inside a homogeneous semitransparent particle can be calculated using the radiative transfer [5,6] or the electromagnetic [14] (EM) theory. Since the former is considerably simpler than the latter, the radiative transfer theory is used to calculate the local radiation field and the local volumetric absorption rate of radiation by a particle. Also, accounting for radiation reflection at an interface or of radiation interreflections inside of the particle is exceedingly difficult using the EM theory.

The radiative transfer equation (RTE) describes the intensity of radiation in the direction of the unit vector (\hat{s}). The intensity is attenuated by absorption and enhanced by emission. Thus, the RTE for the solid-phase in spherical coordinates can be expressed as

$$\mu \frac{\partial I_{\lambda,i}}{\partial r} + \frac{(1 - \mu^2)}{r} \frac{\partial I_{\lambda,i}}{\partial \mu} = \frac{\partial I_{\lambda,i}}{\partial s} = \kappa_{\lambda,i} [I_{b,\lambda}(T_i) - I_{\lambda,i}], \quad i = s, m. \quad (5)$$

The first term on the right-hand-side accounts for emission and the second for absorption of radiation. This equation is subjected to the boundary conditions of which the RTE is considered for heating/melting period.

During the heating period the spectral intensity leaving the solid–gas interface ($r = R$) in the $-\mu$ direction (referred to Fig. 2) is a sum of transmitted and reflected contributions and can be expressed as

$$I_{\lambda,s}(R, -\mu_s) = \tau_{\lambda,s}(\mu^o) I_{\lambda}^o(R, \mu^o) + \rho_{\lambda,s}(\mu_s) I_{\lambda,s}(R, \mu_s), \quad (6)$$

where $\tau_{\lambda,s} = 1 - \rho_{\lambda,s}$ is the directional transmissivity at the solid–gas interface, and $\rho_{\lambda,s}$ is the directional reflectivity which can be evaluated by Fresnel’s law [6]. The intensity

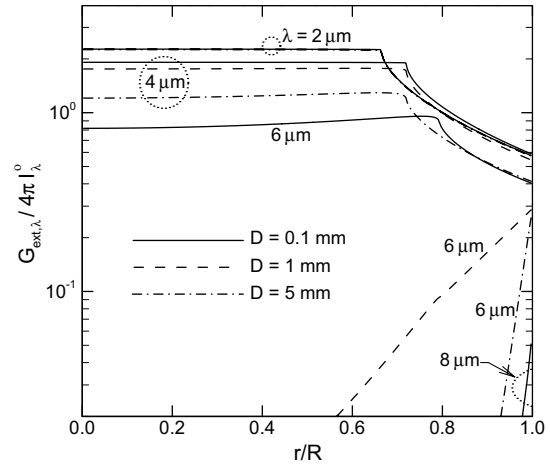


Fig. 2. Spectral distribution of irradiance inside a spherical fused silica particle (in solid-phase) by the external radiation source, $T_{sur} = 2500$ K.

in the direction $-\mu_s$ consists of the transmitted and internal reflected contributions.

The boundary condition at the center of the particle ($r = 0$) is given by

$$I_{\lambda,s}(0, -\mu_s) = I_{\lambda,s}(0, \mu_s). \quad (7)$$

It means that at the center of the particle the radiation field is symmetrical.

During the melting period two interfaces are present: one is formed at the phase-change boundary at the solid–liquid interface, and another is at the liquid–gas interface. The boundary condition for the RTE at the solid–liquid interface ($r = r_f$) is the same as that given by Eq. (6). The directional reflectivity can be evaluated by general Fresnel’s law [15]. In the equation the directional cosine of the solid (μ_s) is related to that in the liquid (μ_m) determined by the Snell’s law [6]

$$n_{\lambda,s} \sin \theta_s = n_{\lambda,m} \sin \theta_m. \quad (8)$$

Since the center ($r = 0$) is still occupied by the solid-phase, the boundary condition is the same as that in the heating period, Eq. (7).

Solution of Eq. (5) with the boundary conditions, Eqs. (6)–(8) and substitution of the resulting equation in the definition of the spectral irradiance, Eq. (2), results in complicated equations for the solid and melt phases; therefore, they are not given here but can be found elsewhere [8]. As an example, the expression for the spectral irradiance in the solid due to external irradiation based on the geometrical optics theory can be written as [8]

$$G_{ext,\lambda}(r) = \int_0^{\theta_{cr}} \frac{\tau_{\lambda}(\theta) \pi I_{\lambda}^o \sin 2\theta}{\zeta^2 \cos \beta} \left[\frac{\exp(-l_1) + \exp(-l_2)}{1 - \rho_{\lambda}(\theta) \exp(-l_3)} \right] d\theta, \quad (9)$$

$$0 \leq r < R,$$

where $\beta = \sin^{-1}[\sin \theta / (n_{\lambda} \zeta)]$, τ_{λ} is the transmissivity defined by $1 - \rho_{\lambda}$ evaluated from Fresnel’s law, and the critical angle θ_{cr} is determined by $\sin \theta_{cr} / n_{\lambda} < \zeta < 1$. The optical distances in Eq. (9) are defined as follows:

$$l_1 = \frac{\tau_{d,\lambda}}{2} \left[\sqrt{1 - (\sin \theta/n_\lambda)^2} - \sqrt{\zeta^2 - (\sin \theta/n_\lambda)^2} \right], \quad (10a)$$

$$l_2 = \frac{\tau_{d,\lambda}}{2} \left[\sqrt{1 - (\sin \theta/n_\lambda)^2} + \sqrt{\zeta^2 - (\sin \theta/n_\lambda)^2} \right], \quad (10b)$$

$$l_3 = \tau_{d,\lambda} \sqrt{1 - (\sin \theta/n_\lambda)^2}. \quad (10c)$$

In the above equations $\tau_{d,\lambda}$ ($=\kappa_\lambda D$) is the spectral optical diameter. Note that in deriving Eq. (9) the emission by the particle has been neglected. With emission accounted for, the expressions for the local spectral irradiances (e.g., $G_{\text{int},\lambda}$) in the solid and melt phases are much more complex. The lengthy derivation details are not provided in this paper but can be found elsewhere [8].

The optical diameter is an important parameter for determining the opacity of a particle. However, the value is not constant but changes as a consequence of melting. The particle can range from being opaque to semitransparent. The dynamics of the process is important in determining the spectral local absorption of radiation in the semitransparent and opaque parts of the spectrum. When the particle is “opaque” to radiation, there is no need to account for radiative transfer in the energy equation but only in the boundary condition.

The spectral irradiance distributions for a fused silica particles are shown in Fig. 2 for external irradiation (no internal emission). For wavelengths having larger optical diameters the irradiance practically vanishes inside the particle and are quite small at the surface as evident in the figure. This indicates that for these wavelengths the particle is effectively opaque. Also, for larger particles, the spectral irradiances in the solid and liquid phases becomes more significant when the internal emission is accounted for [8].

3.1. Method of solution

The energy equation for both preheating and melting periods can be solved by the backward-time (or implicit) centered-space (BTCS) finite differential approximation method [16]. This method is unconditionally stable, and the truncation error is bounded by the order of $O(\Delta t + \Delta r^2)$ [16]. The interface condition, Eq. (4), was satisfied by iteratively solving the equation and determining the velocity (dr/dt) to within the desired accuracy. However, before solving the system of equations, the distribution of the internal volumetric radiant energy absorption rate needs to be calculated.

The spectral internal irradiance, Eq. (9), is calculated using Simpson’s 1/3 rule. The computation is performed as a summation over the spectrum. Thus, the local absorption rate distribution is evaluated by

$$\mathcal{A} = \int_0^\infty \kappa_\lambda G_\lambda d\lambda \simeq \sum_i^M \kappa_{\lambda_i} (G_{\text{ext},\lambda_i} + G_{\text{int},\lambda_i}) \Delta\lambda_i, \quad (11)$$

where M represents the number of spectral increments.

The number of bands M chosen is dependent on the optical diameter of the particle. If the optical diameter corresponding to a given wavelength is much greater than one, the particle is considered to be opaque to radiation for the wavelength. For more accurate evaluation of the local absorption rate, increasing the band number M is inevitable. However, the choice of too large a number of bands is impractical due to excessive computer time requirements. Sensitivity studies were conducted to determine the appropriate time step Δt , the radial increment Δr as well as the number of spectral bands M to obtain numerical results that are independent of these numerical parameters.

4. Results and discussion

4.1. Scope and model parameters

Silicon dioxide or silica (SiO_2) is being widely used in many modern technologically important applications such as fiber-optics, electronics, semiconductors, and material industries [1]. The spectral absorption coefficient of fused silica varies by about eight orders of magnitude in the spectral range between 0.4 and 50 μm [17,18]. For wavelengths greater than 4.5 μm fused silica is strongly absorbing. Owing to its technological importance and the fact that its thermodynamic, thermophysical, and optical properties are well established, fused silica was chosen as an example of a semitransparent material for this study. At high temperature the melting process is significantly affected by internal volumetric absorption and emission of radiant energy. Heating/melting is involved in fused silica processing operations and, therefore, understanding of heat transfer during such operations is required. The thermophysical and optical properties are available; therefore, it is used as an example semitransparent material. Complex index of refraction ($m_\lambda = n_\lambda - ik_\lambda$) data are taken from Palik (0.6 nm–500 μm) [17] and Kashan and Nassif (0.2 μm –3.0 μm) [18]. It is recognized that the refractive index is dependent on temperature as described in the literature [19–21]. However, since the available data are lacking and for simplifying the computation, the index of refraction is assumed to be independent of temperature in the numerical calculations.

Owing to the non-interactive nature of the model (i.e., gas flow outside the particle is not coupled to the particle), convective heat transfer from the ambient gas to the particle and radiative transfer from external radiation source(s) are treated parametrically. A wide range of particle diameters (from 0.1 mm to 10 mm), velocities and temperatures of the ambient gas, and surroundings (radiation sources) temperatures are considered, and results presented and discussed.

4.2. Temperature distributions

A semitransparent particle traps radiant energy inside the particle, and the temperature in the interior of the

particle could be higher than the fusion temperature due to internal absorption of radiation. Since the melting rate depends on the temperature gradients on the both sides of the interface, as shown by Eq. (4), superheating may cause the temperature gradient on the solid side to be negative. This is expected to increase the melting rate.

Figs. 3 and 4 show the temperature distributions during melting for particles of 1 mm and 2 mm diameter particles, respectively. The temperature distributions at earlier times are not given in the figures, because they vary little with the radius, show the expected trends and do not reveal new phenomena. For larger size particles the radiant energy absorbed and emitted is much greater than for small particles. Thus, the instantaneous temperature at the center is much higher than that of small particles. The discontinuities in the temperature gradients in the figures correspond to the interface positions during melting. The profiles have been calculated by accounting for both internal absorption and emission of radiation. No generalizations about the

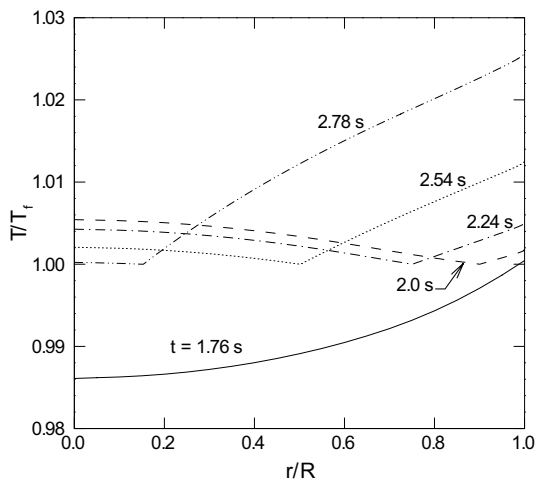


Fig. 3. Temperature distributions of a fused silica particle: $D = 1$ mm, $Re = 0$, $T_0 = 300$ K, $T_f = 1883$ K, and $T_g = T_{sur} = 2500$ K.

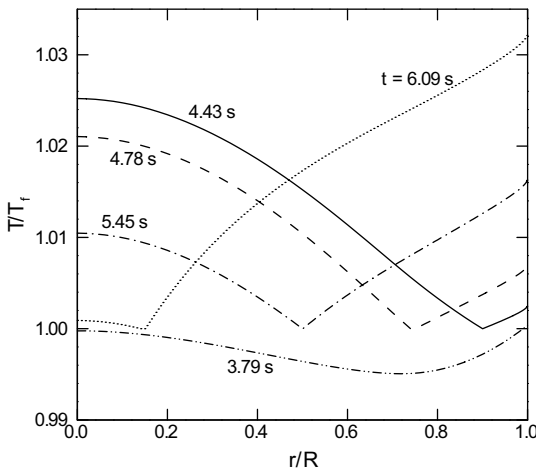


Fig. 4. Temperature distributions of a fused silica particle: $D = 2$ mm, $Re = 0$, $T_0 = 300$ K, $T_f = 1883$ K, and $T_g = T_{sur} = 2500$ K.

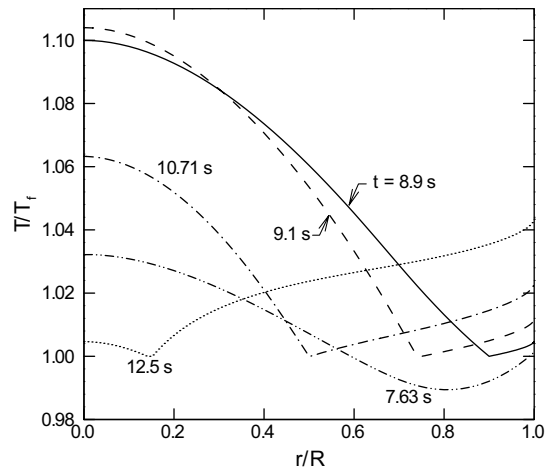


Fig. 5. Temperature distributions of a fused silica particle calculated by Model 5: $D = 5$ mm, $Re = 0$, $T_0 = 300$ K, $T_f = 1883$ K, and $T_g = T_{sur} = 2500$ K.

relative importance of radiation versus convection on the heating and melting of fused silica particles can be made without performing detailed calculations for the specific particle diameter and external flow and heating conditions. Some special cases have been examined and the results of calculations are given elsewhere [8].

Fig. 5 show the temperature distributions during the melting for a 5 mm diameter particle. The interface advances gradually from the surface to the center. Meanwhile, the temperature at the center decreases and finally approaches the fusion temperature. Also, the temperature gradient on the left-hand-side of the interface becomes flatter. Heat transfer in the interior of the particle is dominated by conduction, because the thermal conductivity of fused silica is relatively high and the fact that the spectral opacity of the particle is quite small.

The effect of surroundings temperature on the heating processes of a 10 mm diameter fused silica particle is shown in Fig. 6. Since an increase in the surroundings temperature shifts to the opaque as well as the semitransparent parts of the spectral range of the incident radiation, the temperature has been varied to examine the effect. The figure shows that the core (center) temperature of the particle becomes gradually higher than the surface temperature as the surroundings temperature is increased. This is due to the fact that a larger fraction of the blackbody energy shifts from in the opaque part of the spectrum to in the semitransparent part of the spectrum. In other words, the radiant energy absorbed and emitted by the surface of the particle shifts more to the volume of the particle.

In this work the particle is considered to be suspended as it is being heated to be melted. Thus, the effect of Reynolds number based on the gas free stream velocity and the particle diameter on the heating and melting processes is examined parametrically. A comparison of temperature histories show the effect of the Reynolds number on the heating (given in Fig. 7) and reveal that the surface and

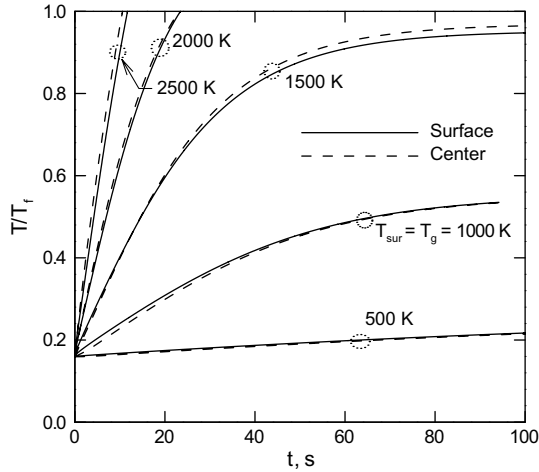


Fig. 6. Effect of surrounding temperature on the heating of a fused silica particle: $D = 10$ mm, $Re = 0$, $T_0 = 300$ K, $T_f = 1883$ K.

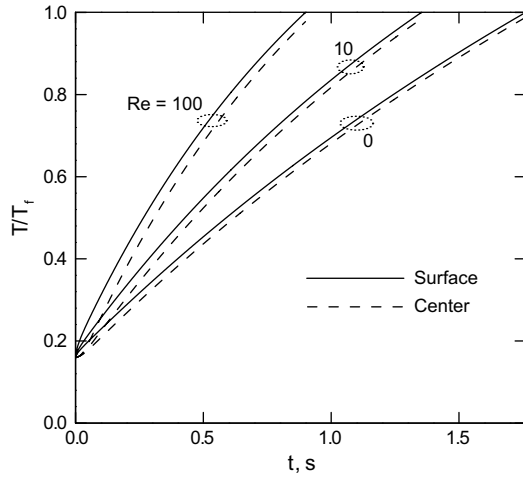


Fig. 7. Temperature histories of a fused silica particle during heating: $D = 1$ mm, $T_0 = 300$ K, $T_f = 1883$ K, and $T_g = T_{sur} = 2500$ K.

the core (center) temperatures are differ more when Reynolds number is larger. This is due to intense heating at the particle surface.

4.3. Interface motion

Fig. 8 shows the effect of Reynolds number on the interface position. As expected, the Reynolds number does not influence the interface position of a larger particle as much as it does the small particle. This is owing to the fact that the average heat transfer coefficient \bar{h} [11] is inversely proportional to D , i.e., $\bar{h} = k\overline{Nu}_D(Re_D)/D \sim 1/D^n$ in which $n = 1$ when the Reynolds number is zero. An attempt has been made to scale the time as t/D^2 in order to collapse the results for all particle diameters to a single curve. This would have been possible in the absence of radiative transfer and/or when heating/melting processes are controlled by diffusion. Unfortunately, the heating/melting processes of the particle are not controlled by diffusion for the condi-

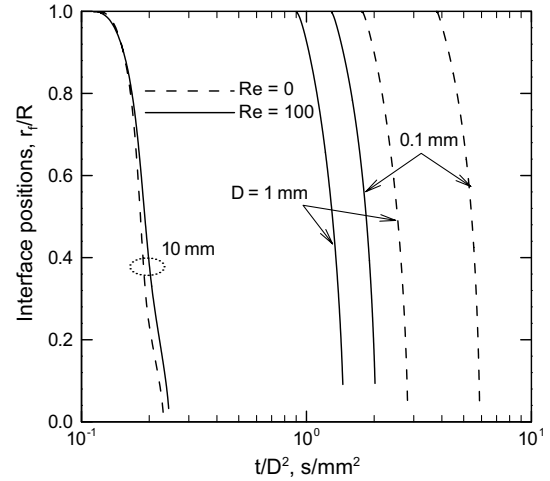


Fig. 8. Effect of convection on the interface positions of a fused silica particle: $T_0 = 300$ K, $T_f = 1883$ K, and $T_g = T_{sur} = 2500$ K.

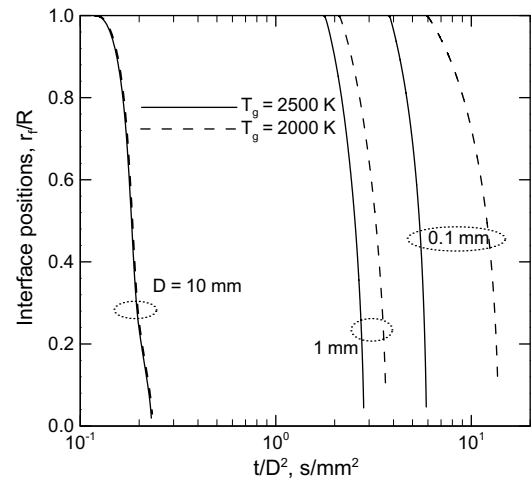


Fig. 9. Effect of gas temperature on the interface positions of a fused silica particle: $Re = 0$, $T_0 = 300$ K, $T_f = 1883$ K, $T_{sur} = 2500$ K.

tions considered, and the curves for different size particles do not collapse to a single set.

The effect of gas temperature on the heating and melting processes of a fused silica particle is illustrated in Fig. 9. The results show trends in the interface positions with the change in the gas temperature. A decrease in the gas temperature T_g results in a decrease in the convective heat flux and, therefore, a decrease in the melting rate, all other parameters being equal.

4.4. Heat transfer

A comparison of the convective and the surface radiative heat fluxes at the particle surface is shown in Fig. 10. Both the convective heat flux and the net surface radiative heat flux decrease as time increases, because the surface temperature increases during the heating process. The figure reveals that convective heat flux is higher than the

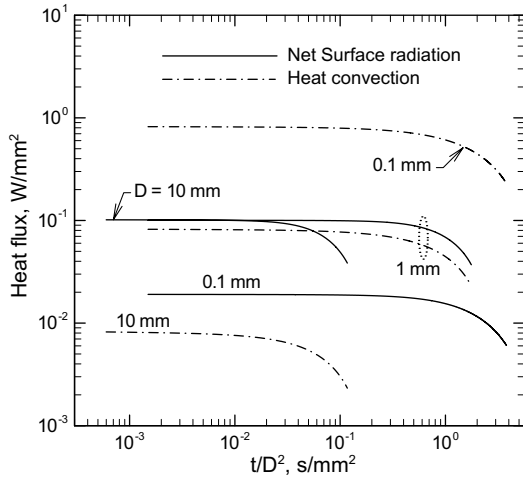


Fig. 10. Effect of particle diameter on the surface heat flux of fused silica particles during the heating period: $Re = 0$, $T_0 = 300$ K, $T_f = 1883$ K, and $T_g = T_{sur} = 2500$ K.

net surface radiation for smaller particles. This indicates that convection dominates the heat transfer rate when the particles are small. The figure shows that the net surface radiative flux for $D = 1$ mm is close to that for 10 mm. This is due to the fact that the opaque parts of the spectrum for 1 mm and 10 mm particle are close to each other.

The effect of Reynolds number on the heat transfer rate is shown in Figs. 11 and 12 for $D = 0.1$ mm and $D = 10$ mm, respectively. The two figures show that increasing the Reynolds number reduces the surface heat transfer rate. For small particles (as shown in Fig. 11) convection dominates the surface heat transfer rate. Thus, the surface radiation and the internal radiative transfer rates are affected by convection due to the surface temperature being significantly affected by convection. For large SiO_2 particles (as shown in Fig. 12) increasing the Reynolds number does not greatly affect the heat transfer rate.

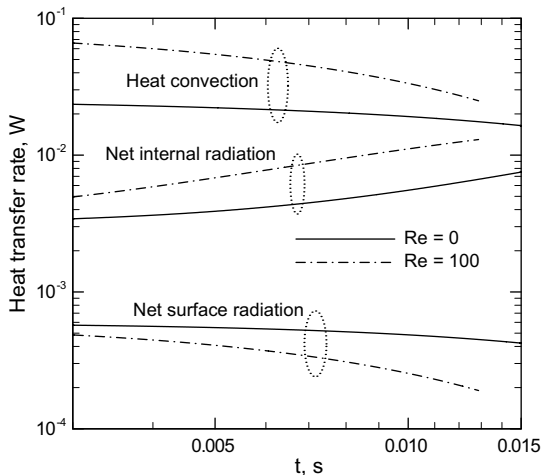


Fig. 11. Heat transfer rate of fused silica particles during the heating period: $D = 0.1$ mm, $T_0 = 300$ K, $T_f = 1883$ K, and $T_g = T_{sur} = 2500$ K.

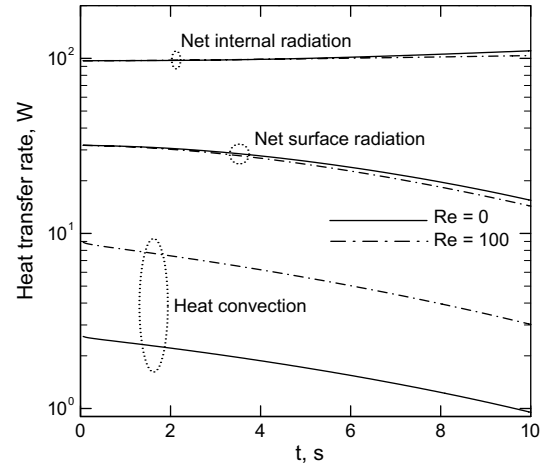


Fig. 12. Heat transfer rate of fused silica particles during the heating period: $D = 10$ mm, $T_0 = 300$ K, $T_f = 1883$ K, and $T_g = T_{sur} = 2500$ K.

Since a semitransparent particle traps radiant energy within the particle, the temperature in the interior of the particle could be higher than the fusion temperature due to internal absorption of radiation. Hence, the melting rate is dependent on the temperature gradients on both sides of the interface, as shown by Eq. (3). Superheating may cause the temperature gradient on the solid side to be negative. This increases the melting rate.

5. Concluding remarks

The heating and melting of a semitransparent SiO_2 particle has been formulated by developing a model to describe the heating/melting of a fused silica particle as an example. The effect of absorption and emission of radiation was considered. Because a semitransparent particle traps radiant energy inside the particle, the temperature in the interior of the particle can be higher than the fusion temperature due to internal absorption of radiation. Since melting rate is dependent on the temperature gradients on both sides of the interface, superheating may cause the temperature gradient on the solid-phase side to be negative. This increases (or enhances) the melting rate. Based on the results obtained, the conclusions from the results of the numerical simulations can be summarized as follows:

- Absorption of external radiation strongly affects the heating and melting processes of a fused silica particle. Emission of radiation becomes significant when the temperature of the particle is sufficiently high. The surroundings temperature significantly influences the heating and melting processes since it affects the radiant energy distribution in the opaque and in the semitransparent parts of the spectrum. Therefore, the surroundings temperature is expected to impact the radiation absorption in the semitransparent part of the spectrum and cause the internal temperature to be higher than the fusion temperature (overheating) resulting in an increased melting rate.

- Absorption and emission of radiation are not important for very small size fused silica particles ($D < 1$ mm). This is because convective heat transfer predominates over radiation during the heating/melting of the small particles. When convective heat transfer to the particle predominates over radiation ($D < 1$ mm), increasing the convective heat flux by either increasing the ambient gas velocity and/or ambient gas temperature, enhances the melting rate, but for larger particles when radiation predominates over convection the heating/melting rate is affected little by convection.
- No generalization about the relative importance of radiative transfer in the heating/melting of a semitransparent particle can be reached based on the results obtained for fused silica. Detailed calculations would have to be made for the specific material, its thermodynamic, thermophysical, and radiation properties, particle diameter and imposed external flow and heating conditions.
- No published experimental data could be identified in the literature; therefore, the model validation remains a task for the future.
- The assumption that there is no interaction between the external gas flow field and the melting particle needs to be relaxed, and this remains a significant task for the future.

References

- [1] Y.P. Wan, V. Prasad, G.-X. Wang, S. Sampath, J.R. Fincke, Model and powder particle heating, melting, resolidification, and evaporation in plasma spraying processes, *J. Heat Transfer* 121 (1999) 691–699.
- [2] A. Anselmo, V. Prasad, J. Koziol, K.P. Gupta, Numerical and experimental study of a solid pellet feed continuous Czochralski growth process for silicon single crystals, *J. Cryst. Growth* 131 (1993) 247–264.
- [3] J. Chung, S. Ko, N.R. Bieri, C.P. Grigoropoulos, D. Poulikakos, Conductor microstructures by laser curing of printed gold nanoparticle ink, *Appl. Phys. Lett.* 84 (5) (2004) 801–803.
- [4] F. Oeters, *Metallurgy of Steelmaking*, Verlag Stahleisen, Dusseldorf, 1994.
- [5] R. Viskanta, E.E. Anderson, Heat transfer in semitransparent solids, in: J.P. Hartnett, T.F. Irvine, Y.I. Cho (Eds.), *Advances in Heat Transfer*, 11, Academic Press, New York, 1975, pp. 317–441.
- [6] M.F. Modest, *Radiative Transfer*, second ed., Academic Press, New York, 2003.
- [7] S. Fujino, C. Hwang, K. Fukuoka, Density, surface tension, and viscosity of $\text{PbO-B}_2\text{O}_3\text{-SiO}_2$ glass melts, *J. Am. Ceram. Soc.* 87 (1) (2004) 10–16.
- [8] C.C. Tseng, Phase change in semitransparent droplets and particles heated by convection and radiation, Ph.D. thesis, Purdue University, West Lafayette, IN, 2005.
- [9] L.H. Liu, H.P. Tan, T.W. Tong, Transient coupled radiation-conduction in semitransparent spherical particle, *J. Thermophys. Heat Transfer* 16 (1) (2002) 43–49.
- [10] L.H. Liu, H.P. Tan, T.W. Tong, Internal distribution of radiation absorption in a semitransparent spherical particle, *J. Quant. Spectrosc. Radiat. Transfer* 72 (2002) 747–756.
- [11] F.P. Incropera, D.P. DeWitt, *Fundamentals of Heat and Mass Transfer*, fourth ed., John Wiley & Sons, New York, 1996.
- [12] B. Abramzon, W.A. Sirignano, Droplet vaporization model for spray combustion calculations, *Int. J. Heat Mass Transfer* 32 (9) (1989) 1605–1618.
- [13] C.C. Tseng, R. Viskanta, On the hypothesis of internal phase change, *Int. Commun. Heat Mass Transfer* 32 (2005) 1267–1272.
- [14] A. Tuntomo, C.L. Tien, S.H. Park, Internal distribution of radiant absorption in a spherical particle, *J. Heat Transfer* 113 (1991) 407–412.
- [15] M. Born, E. Wolf, *Principles of Optics: Electromagnetic Theory of Propagation, Interference and Diffraction of Light*, seventh (expanded) ed., Cambridge University Press, 1999.
- [16] J.D. Hoffman, *Numerical Methods for Engineering and Scientists*, McGraw-Hill, New York, 1992.
- [17] E.D. Palik, *Handbook of Optical Constants of Solids*, Academic Press, New York, 1985, pp. 749–763.
- [18] M.A. Khashan, A.Y. Nassif, Dispersion of the optical constants of quartz and polymethyl methacrylate glasses in a wide spectral range: 0.2–3 μm , *Opt. Commun.* 188 (2001) 129–139.
- [19] A.A. Higazy, A. Hussein, M.A. Ewaida, M. El-Hofy, The effect of temperature on the optical absorption edge of the titanium oxide-doped soda-lime silica glasses, *Mater. Sci. Lett.* 7 (1988) 453–456.
- [20] N.M. Ravindra, S. Abedrabbo, W. Chen, F.M. Tong, A.K. Nanda, A.C. Speranza, Temperature-dependent emissivity of silicon-related materials and structures, *IEEE Trans. Semiconductor Manuf.* 11 (1) (1998) 30–39.
- [21] M. Modreanu, N. Tomozeiu, P. Cosmin, M. Gartner, Optical properties of LPCVD silicon oxynitride, *Thin Solid Films* 337 (1999) 82–84.